Visual Acuity for Moving Objects in First- and Second-Order Neurons of the Fly Compound Eye

MIKKO JUUSOLA AND ANDREW S. FRENCH
Department of Physiology and Biophysics, Dalhousie University, Halifax, Nova Scotia B3H 4H7, Canada; and Department of Physiology, University of Oulu, 90220 Oulu, Finland

Juusola, Mikko and Andrew S. French. Visual acuity for moving objects in first- and second-order neurons of the fly compound eye. *J. Neurophysiol.* 77: 1487–1495, 1997. The early stages of visual systems contain a variety of components that limit both the spatial resolution and the temporal resolution of vision. When an animal sees a moving object, or moves relative to its environment, both spatial and temporal factors contribute to its ability to resolve the movement. In the present work we have combined currently available knowledge about the early stages of fly vision (optical system, photoreceptors, and large monopolar cells) to predict the resolution of the first two cell layers to moving point objects. These calculations included recent measurements of nonlinear light responses. Because background light level has a strong effect on the temporal behavior of these early visual layers, we examined the effects of light level on motion resolution. We also studied the effect of position within the eye, which is known to affect the static resolution of vision. Our results indicate that responses in large monopolar cells to moving point objects are maximal at angular velocities of 100–200°/s. The resolution of point objects by both these early stages of the visual system is similar from stationary to an angular velocity of ~200°/s. Above this, resolution deteriorates approximately linearly with velocity.

INTRODUCTION

Visual systems often detect and respond to objects that move relative to the animal itself. The fly is a well-known example that can follow moving objects and also move rapidly relative to its physical environment. Although the visual acuity and time-dependent properties of photoreceptors and their postsynaptic neurons have been studied intensively in many species, most studies of motion detection in the fly, and other animals, have emphasized behavioral measures such as orientation and tracking, or movement-detecting neurons that are several synapses beyond the photoreceptors (e.g., Egelhaaf et al. 1988; Reichardt and Poggio 1976; Wehrhahn 1985).

In a theoretical study, Srinivasan and Bernard (1975) estimated the resolution of photoreceptors in compound eyes for moving point objects. They combined the known optical properties of the rhabdomes with the photoreceptor flash responses that were available. Now, twenty years later, we have much more complete data on the time-dependent properties of photoreceptors and large monopolar cells (LMCs), the second-order neurons of compound eyes. In particular, we have recently presented accurate models of the dynamic performance of fly photoreceptors and LMCs that include nonlinear behavior and changes with light adaptation level (Juusola et al. 1995b). In addition, data are available on the acceptance angles of fly photoreceptors as a function of both light adaptation and position across the surface of the eye (Hardie 1979). We now reexamine the abilities of fly photoreceptors and LMCs to detect moving objects.

Light-adapted fly photoreceptors behave approximately linearly, but LMC voltage responses are always nonlinear. Both can be modeled with low error by a second-order Volterra series expansion (Juusola et al. 1995b) with the photoreceptor second-order kernel being zero. With the use of these models, we calculated the voltage responses in photoreceptors and LMCs with the use of digital convolution of the Gaussian light acceptance functions with Volterra expansions obtained from white noise stimulation at a range of background light intensities and constant contrast amplitude.

In the present study, two methods were used to estimate the resolution of photoreceptors and LMCs for positive moving point objects. The first used the width at half-peak amplitude (half-width) of the spatial intensity function produced by a point object moving at constant angular velocity, assuming that moving objects spaced more closely together than the half-width would not be resolved. The second calculated the minimum angular separation required to resolve a pair of point objects moving together at constant angular velocity.

The two approaches produced similar results, with LMCs having slightly better resolution because of their faster temporal responses. Both cell types displayed two regions of behavior. At low velocities, resolution was dominated by the angular sensitivity of the light-accepting components. Above a threshold velocity, the temporal response dominated the resolution, which deteriorated monotonically with increasing velocity.

METHODS

Experimental data

All of the data describing the linear and nonlinear temporal properties of fly photoreceptors and LMCs that were used here have been published before (Juusola et al. 1995b), together with the methods used in the original recordings and the analysis techniques for obtaining the Volterra kernels. Only a brief summary of these measurements is given here.

Flies (*Calliphora vicina*) were stimulated with a green light-emitting diode during intracellular recording from photoreceptors and LMCs. The light stimulus was a pseudorandom signal superimposed on a constant background to produce a contrast signal of constant variance, independent of background. Photoreceptor and LMC recordings were obtained at eight different background light levels (BL1–BL8) corresponding to light intensities

of 160, 500, 1,600, 5,000, 16,000, 50,000, 160,000, and 500,000 effective photons per second in a typical photoreceptor. All of the temporal data used here were obtained from single, high-quality recordings of one photoreceptor cell and one LMC (Juusola et al. 1995b).

Input-output relationships for photoreceptors and photoreceptor-LMC combinations were modeled by a Volterra series of the form

$$y(t) = k_0 + \sum_{\tau=0}^{T} k_1(\tau)x(t-\tau) + \sum_{\tau_1=0}^{T}\sum_{\tau_2=0}^{T} k_2(\tau_1,\tau_2)x(t-\tau_1)x(t-\tau_2) \quad (1)$$

where $x(t)$ and $y(t)$ were the input and output signals as functions of time t, and k_0, $k_1(\tau)$, and $k_2(\tau_1,\tau_2)$ were the zero-, first-, and symmetrical second-order kernels, respectively. The system memory was assumed to last until a maximum lag of T. The kernels were estimated by the parallel cascade method (Korenberg 1982, 1991) with the use of second-order polynomial functions. The kernels obtained were very nearly least-squares estimates, and because a Gaussian input was used, k_1 and k_2 were estimates of the first- and second-order Wiener kernels, respectively.

All calculations and simulations were performed by custom-written programs with the use of the ''C'' language on a personal computer. Double-precision floating point resolution (24-bit mantissa) was used throughout.

Model structure

Fig. 1 illustrates the approach used to calculate the voltage responses in photoreceptors and LMCs to a point object moving across the visual field. The light-accepting properties of the optical components before the photoreceptors in insect compound eyes are usually approximated by a Gaussian function (Götz 1964, 1965). A history of the Gaussian approximation and some theoretical justifications are provided by Warrant and McIntyre (1993). The Gaussian function is actually a function of two-dimensional space across the surface of the eye, but all of the calculations here are based on movements at constant velocity in one dimension across the eye for simplicity, and therefore a Gaussian function of one spatial dimension was used (Srinivasan and Bernard 1975).

For the present work, we used stimuli consisting of point objects (Srinivasan and Bernard 1975), defined as positive Dirac delta functions of unit light contrast. As a point object moves at constant angular velocity W across the visual field of the eye, the Gaussian approximation predicts that the change in light intensity passing through each facet and falling on the rhabdome will be given by

$$f(t) = \exp(-\beta t^2), \quad \beta = (2W/\rho)^2 ln2 \quad (2)$$

where t is the time relative to the instant at which the point object is directly above the optical axis of the facet, and ρ is the width of the Gaussian function at half-amplitude.

Light-adapted fly photoreceptors produce changes in membrane potential that are approximately linear functions of light intensity (French 1980a,b; French and Järvilehto 1978a; Juusola et al. 1994) and can be characterized by an impulse response function, or first-order kernel, $k_{1,\mathrm{pho}}(\tau)$, at each level of light adaptation (Juusola et al. 1995b) with a mean square error of ~3% at background levels BL6-BL8, where the signal to noise level is high. Therefore the predicted photoreceptor response to a moving point object was obtained by digital convolution of the appropriate Gaussian functions with the first-order kernels reported in Juusola et al. (1995b)

$$\nu_{\mathrm{pho}}(t) = \sum_{\tau=0}^{T} k_{1,\mathrm{pho}}(\tau) f(t-\tau) \quad (3)$$

LMCs receive histaminergic synaptic inputs from photoreceptors (Hardie 1989) and hyperpolarize in response to depolarization in photoreceptors (Järvilehto and Zettler 1970; Shaw 1984). Unlike photoreceptor responses, LMC responses are clearly nonlinear under most stimulus conditions (French and Järvilehto 1978b; Juusola et al. 1995a; Laughlin et al. 1987). However, the relationship between light intensity fluctuations and LMC responses was well approximated by a second-order Volterra series or by an LNLN cascade model, where L represents a linear component with memory and N represents a static polynomial nonlinearity. Both models gave mean square error values <10% at background levels BL4-BL8 (Juusola et al. 1995b). Here, the response in an LMC to a moving point object was calculated by passing the Gaussian function through the second-order Volterra series, with the use of first- and second-order digital convolution

$$\nu_{\mathrm{LMC}}(t) = \sum_{\tau=0}^{T} k_{1,\mathrm{LMC}}(\tau) f(t-\tau) + \sum_{\tau_1=0}^{T}\sum_{\tau_2=0}^{T} k_{2,\mathrm{LMC}}(\tau_1,\tau_2) f(t-\tau_1) f(t-\tau_2) \quad (4)$$

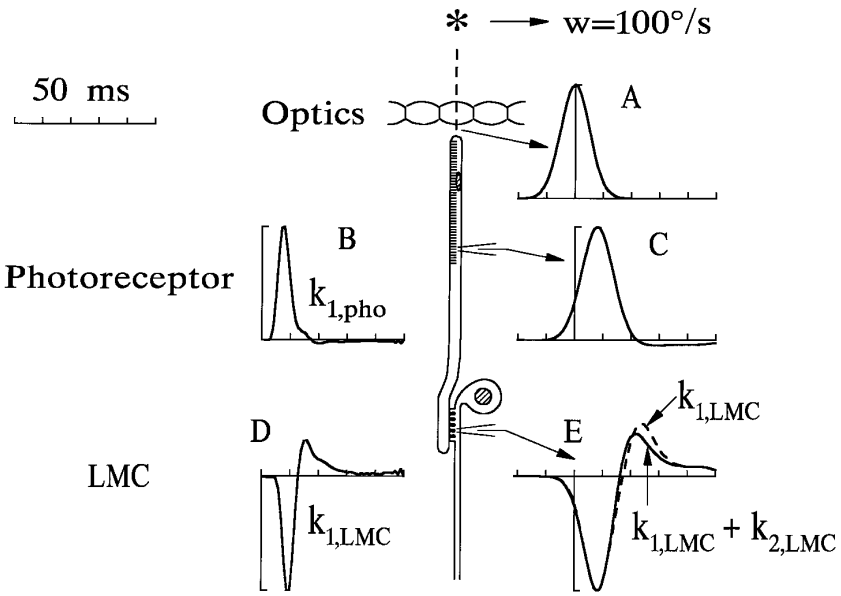

FIG. 1. Calculation of cellular responses to a point object (*) moving across the visual field. The stimulus and optics produced a Gaussian change in light intensity with time at the input of the photoreceptor (A). This function was then convolved with the impulse response, or 1st-order kernel, $k_{1,\mathrm{pho}}(\tau)$, of the photoreceptor (B), to produce the photoreceptor signal (C). The response in the 2nd-order large monopolar cell (LMC) was obtained by passing the Gaussian function through a nonlinear Volterra series consisting of 1st-order [D; $k_{1,\mathrm{LMC}}(\tau)$] and 2nd-order [$k_{2,\mathrm{LMC}}(\tau_1,\tau_2)$] kernels. The figure illustrates an angular velocity of 100°/s and background level BL8. The LMC response (E) is shown both with and without the 2nd-order nonlinear term.

Figure 1 illustrates the responses at each stage of the model with a single point object moving at 100°/s across the eye, including the effect of omitting the second-order kernel from the calculations for the LMC response.

Angular sensitivity

The angular sensitivities of *Calliphora* photoreceptors (R1–6) have been measured as a function of facet position relative to the anterior-posterior axis of the eye (Hardie 1979). The data were reported as the width of the angular sensitivity function at half-maximum amplitude, ρ. Inspection of the data shows that for dark-adapted eyes, ρ was ~1.5° for all facet positions up to 30° from the front of the eye, and then increased approximately linearly to a maximum of 2.5° at 140° from the front of the eye. Light adaptation reduced the half-width to a minimum of 80% of the dark-adapted value. For simplicity, we used a Gaussian function to describe the angular sensitivity and parameterized the data with the use of a linear relationship between distance from the front of the eye and Gaussian half-width, assuming that light adaptation decreased the half-width linearly. These parameterizations are illustrated in Fig. 2, together with examples of the Gaussian functions under several different conditions. These parameters were used in all calculations.

Kernel values

The responses of photoreceptors and LMCs to light were described by Volterra functional expansions (*Eq. 1* and Marmarelis and Marmarelis 1978) with the use of data obtained previously by stimulating with a pseudorandomly modulated light intensity superimposed on a constant light background to give a constant contrast amplitude at each background level (Juusola et al. 1995b). For photoreceptors, only the first-order kernel, or flash response, was used, because this was previously found to fit the experimental data with <10% mean square error, and no significant improvement was obtained by adding the second-order term. For LMCs, inclusion of the second-order kernel gave a significant improvement in fitting the data, so both terms were used here. The first-order kernels for each background light intensity, together with the second-order kernels at BL8, are shown in Fig. 3. Note that LMCs hyperpolarize in response to light, as described above. Responses in both cell types increased and became faster with light adaptation. Note the amplification occurring between the photoreceptors and the LMCs.

RESULTS

Temporal responses to a single moving point object

Predicted peak responses to a moving point object in single photoreceptors and LMCs as functions of angular velocity are shown in Fig. 4 for the minimum and maximum light levels. Note again that LMCs hyperpolarize in response to light, so that the peak response corresponds to the maximum negative deflection. These calculations were made for cells at the front of the eye (0° from the fovea). As an object moves more rapidly across the visual field, it provides a more rapidly changing input to the photoreceptors. Because photoreceptors are approximately low-pass filters (French 1980a,b), their responses were relatively constant at low velocities, but decreased above ~100°/s. However, LMCs have more band-pass characteristics, and so responded maximally to moving objects. The angular velocity producing the greatest response increased from ~100 to 200°/s with increasing background light intensity.

Another difference between photoreceptors and LMCs was the range of responses observed at different light intensities. Although increasing the background level from BL1 to BL8 produced an increase of >20-fold in photoreceptor response, the same change produced an increase of <4-fold in LMC response.

Spatial responses to a single moving point object

As a single point object moves across the visual field of a compound eye, a response occurs in each photoreceptor that receives light from the object. If the photoreceptors were regularly spaced, with infinitely high angular resolution, we could calculate a spatial distribution of photoreceptor responses

$$V_{\text{pho}}(\phi, t) = \nu_{\text{pho}}(t - \phi/W) \quad (5)$$

where ϕ is the angular distance from the photoreceptor immediately below the moving point object. This function is the same as the temporal response in the photoreceptor, but with the spatial dimension, ϕ, having the opposite sign

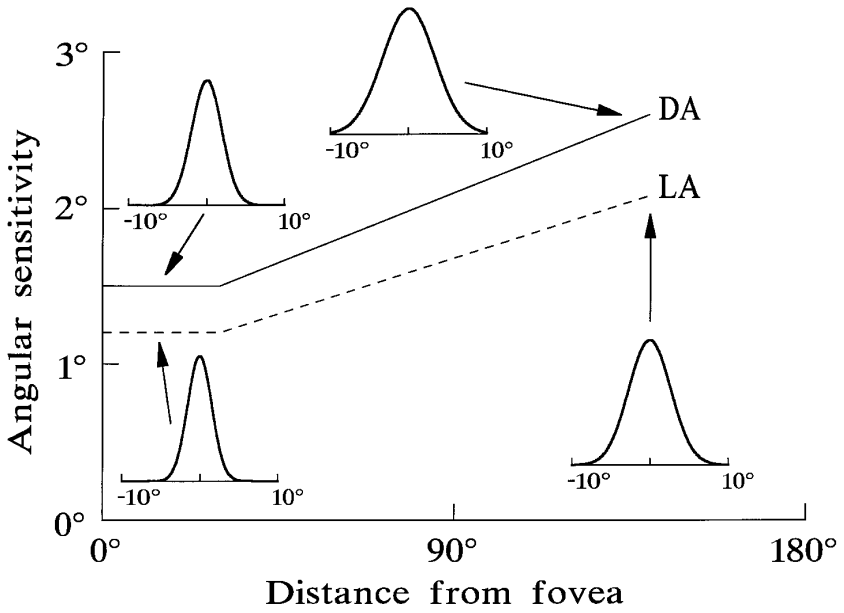

FIG. 2. Angular sensitivity function of the optics was modeled as a Gaussian function whose width varied linearly with light adaptation (background level) and linearly with position in the eye beyond 30° from the fovea (see text). Ordinate: half-width of the angular sensitivity function at half-maximum amplitude. The parameters were taken from the original measurement of Hardie (1979). DA, dark adapted; LA, light adapted.

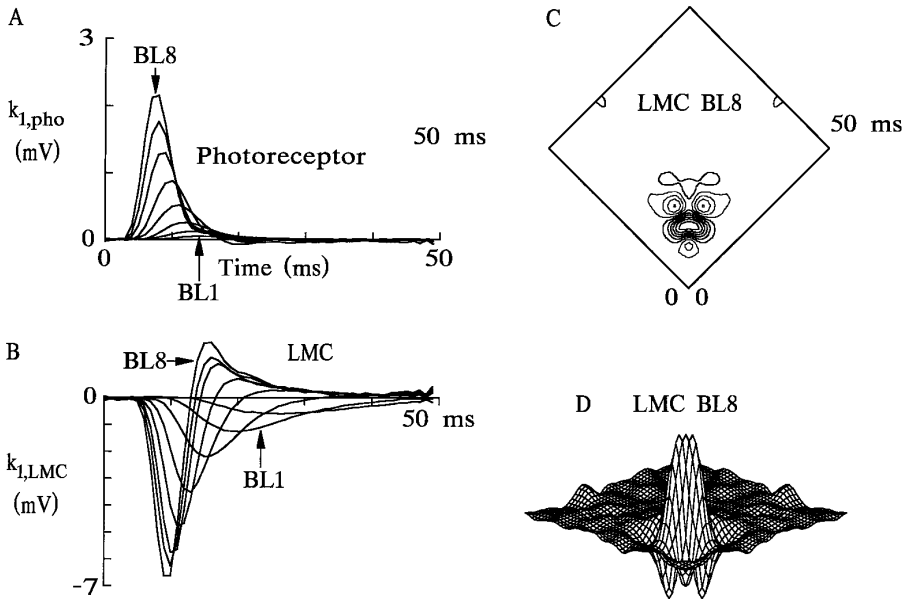

FIG. 3. Temporal responses of photoreceptors and LMCs were taken from our previously published data (Juusola et al. 1995a,b). Photoreceptors were characterized entirely by the 1st term in a Volterra kernel expansion, $k_{1,pho}(\tau)$, shown at the 8 different background levels, BL1–BL8 (*A*). LMCs were characterized by the 1st 2 terms in a Volterra kernel expansion [*B;* $k_{1,LMC}(\tau)$, and *C* and *D;* $k_{2,LMC}(\tau_1,\tau_2)$]. $k_{1,LMC}(\tau)$ is shown for levels BL1–BL8 and $k_{2,LMC}(\tau_1,\tau_2)$ is shown at BL8 with the use of both contour (*C*) and perspective (*D*) plots.

to time, and varying with velocity, *W*, as well as time. An example of this function in which discrete time and space resolutions of 1 ms and 0.2° are used is illustrated in Fig. 5, together with a similar calculation for the LMCs. The moving point object creates spatial waves of voltage changes in the photoreceptors and LMCs, most of which lag behind the object itself. The small parts of the responses that lead the object are caused by the angular acceptance of the optical system, which means that a photoreceptor begins to receive light from the object before it is directly overhead.

Spatial responses for a range of angular velocities of a moving point object are shown as gray-scale intensities (Fig. 6). In these plots, responses similar to those of Fig. 5 were used to create a gray scale of 10 levels at each velocity, and then the gray scales were converted to random dot densities. The plots show the responses produced across the surface of the eye by a moving dot at the instant it passed the central point. Because LMC responses are predominantly hyperpolarizing, they were inverted. Only positive values are shown in both the photoreceptor and LMC plots. Note the large angular shifts produced by high velocities.

Because the forms of the spatial responses are simple transforms of the temporal responses, their widths at half-maximum amplitude, or spatial half-widths, $sP(W)$ and $sL(W)$ (Fig. 5), could be obtained directly from the temporal half-widths, $tP(W)$ and $tL(W)$, of the photoreceptors and LMCs

$$sP(W) = tP(W), \quad sL(W) = tL(W)W \tag{6}$$

The temporal responses were directly available from the model, so the spatial half-widths were calculated without the need to calculate the spatial responses, and without requiring any assumptions about receptor spacing. Spatial half-widths for photoreceptors and LMCs were calculated for a

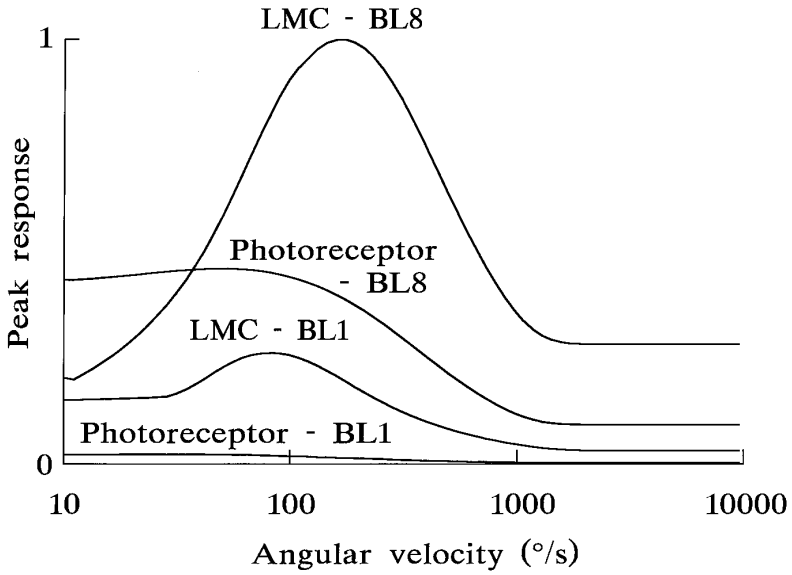

FIG. 4. Calculated peak responses of photoreceptors and LMCs to a point object moving across the visual field at a range of angular velocities. Responses are shown at the lowest (BL1) and highest (BL8) background intensities, for cells at the front of the eye. All results have been normalized to the maximum peak response in LMCs at BL8.

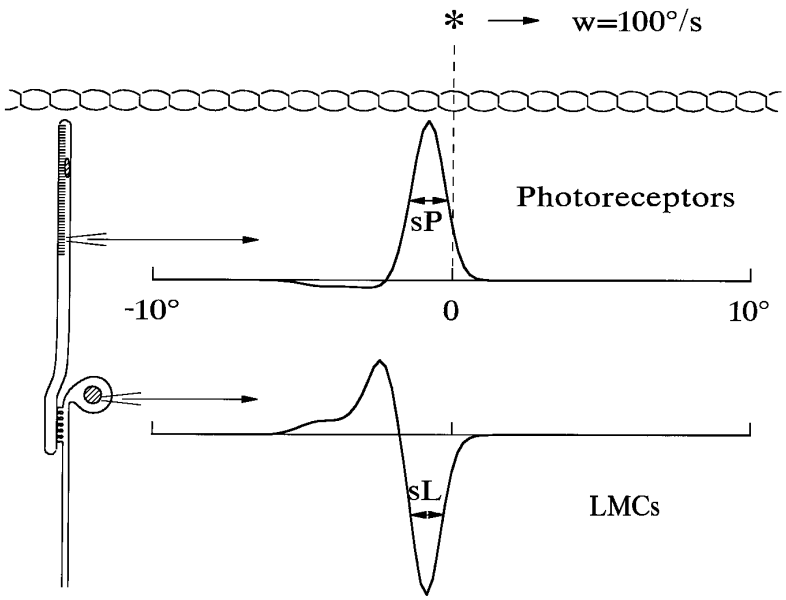

FIG. 5. Object moving across the visual field causes responses in the photoreceptors and LMCs that produce a spatial pattern resembling a reversed temporal response in a single cell. Calculated responses are shown for an object moving at 100°/s and at BL8. The widths of the spatial responses increased with velocity, and were characterized as spatial half-widths, *sP* (photoreceptors) and *sL* (LMCs). Responses of photoreceptors and LMCs in Figs. 5–8 have all been normalized to the peak values.

range of velocities, background levels, and positions relative to the front of the eye.

Spatial responses to a pair of moving point objects

When a pair of point objects move across the visual field, combined responses are produced in the photoreceptors and LMCs that produce corresponding spatial responses (Fig. 7). Because the photoreceptor temporal responses were modeled linearly, their spatial responses were simply the summed responses to the two separate objects. However, LMC responses were nonlinear, so their temporal and spatial responses to a pair of objects were not simple summations of the separate responses to single objects (Fig. 7).

Responses to pairs of objects were calculated for the same range of conditions as spatial half-widths. In each case, the angular separation between the pair of objects was increased from zero in steps of 0.2° until the dip between the two peak responses was 19% of the smaller peak (measured from the baseline of 0 V). This corresponds to a spatial version of the Rayleigh criterion for diffraction-limited resolution of two point objects by an optical system (Goodman 1968). This value was used as a measure of the spatial resolution of the cell layer to a pair of moving point objects (Fig. 7).

Spatial resolution

Figure 8 shows the calculated values of spatial half-width and minimum separation of pairs of point objects (2 points) at background level BL8 as a function of angular velocity. Note the strong agreement between the results obtained by the two different methods of estimating the resolution of moving point objects. There is also good agreement between the resolutions obtained for the photoreceptors and LMCs, with the LMCs having slightly better resolution for more rapidly moving objects.

All of the curves show two distinct regions of behavior. At low angular velocities, below ~200°/s, the resolution is <2°, independent of velocity, but above this threshold, the resolution deteriorates. The spatial half-width, or minimum

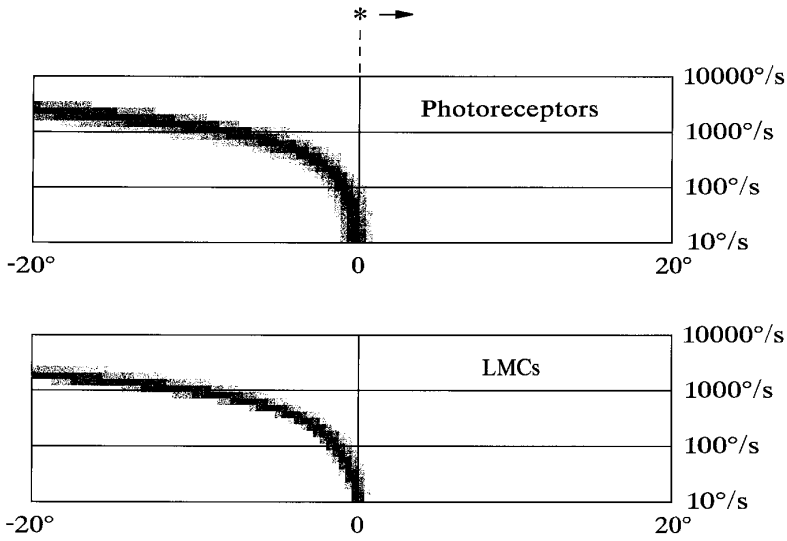

FIG. 6. Calculated responses of photoreceptors and LMCs to a moving point object are shown as intensity plots, with the use of randomly scattered dots and a range of 10 levels for each normalized response. The responses are shown for a range of angular frequencies, at a constant background light intensity (BL8) and for cells at the front of the eye. LMC responses were inverted in sign and negative responses are not shown.

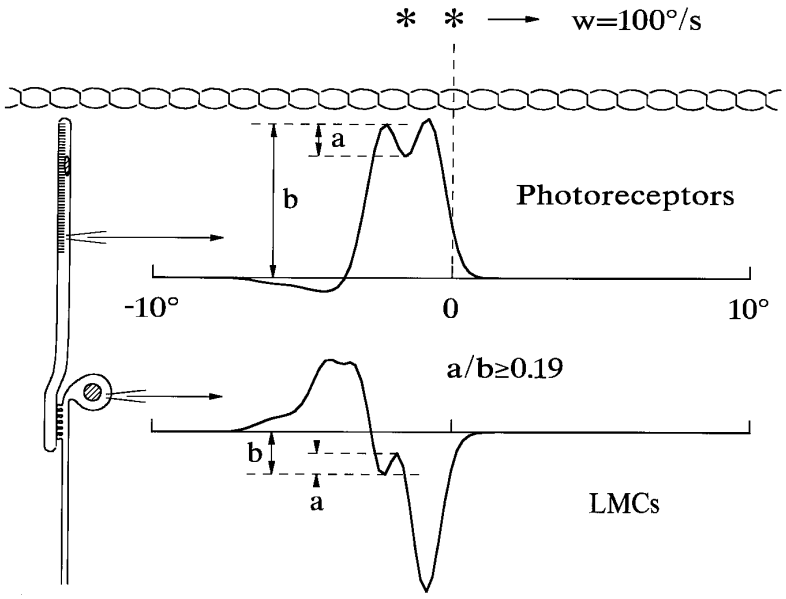

FIG. 7. Pair of moving objects produces a fused spatial response if the objects are sufficiently close together. In the present model, the photoreceptors were represented by a linear function, so that the fused response was the sum of the 2 individual responses. However, the LMC fused response was a nonlinear combination of the separate responses. The criterion used for detecting 2 objects as separate entities was that the dip between the 2 peaks was ≥19% of the lowest peak, measured from the baseline.

separation, increases approximately linearly with angular velocity and the slope of this increase is ~5 ms, as expected from the temporal half-widths of the photoreceptor and LMC responses.

For other calculations, we compared the behavior at two angular velocities of 100°/s and 1,000°/s, which are distinctly below and above the threshold velocity of 200°/s for the change in response behavior for moving point objects. We also used only the spatial half-widths as measures of resolution, because they were simpler to calculate and required no assumptions about physical resolution. This decision was based on the close agreement between the results of the two different methods (Fig. 8).

As background light intensity increased, the responses of both photoreceptors and LMCs became faster, but the change in LMCs was more profound (Fig. 3). This caused an improvement in the resolution of moving objects at high velocities that was also more pronounced in LMCs (Fig. 9). At low velocities, changing the level of light adaptation had comparatively little effect on the resolution of photoreceptors or LMCs. Even at high levels of light adaptation, both types of cells resolved slowly moving objects significantly better than rapidly moving objects.

In contrast to the effects of light adaptation, variation in the angular acceptance of the photoreceptors had more effect at low velocities. With movement away from the fovea, or front of the eye, the angular acceptance of the facets widens and this increased the spatial half-width of the response to a moving point object (Fig. 10). However, the responses of photoreceptors and LMCs to rapidly moving objects were much less affected by this change and displayed an approxi-

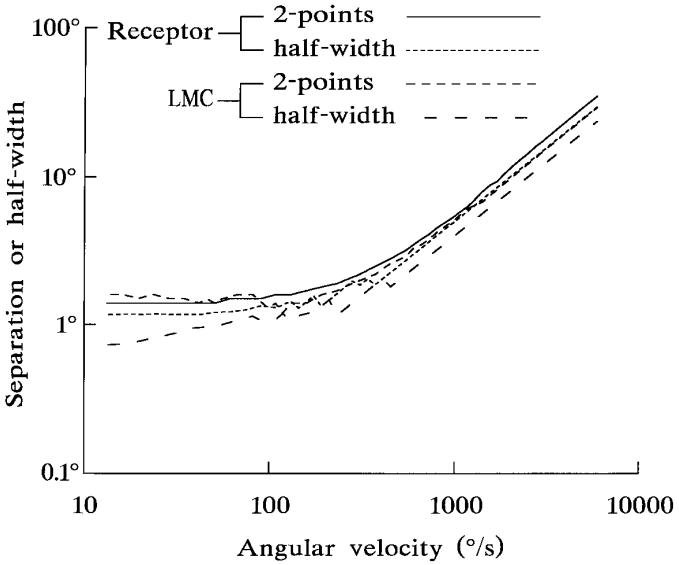

FIG. 8. Spatial half-widths and minimum separations were calculated for pairs of objects moving at a range of angular velocities across the eye. This figure shows these results at background level BL8 for both photoreceptors and LMCs.

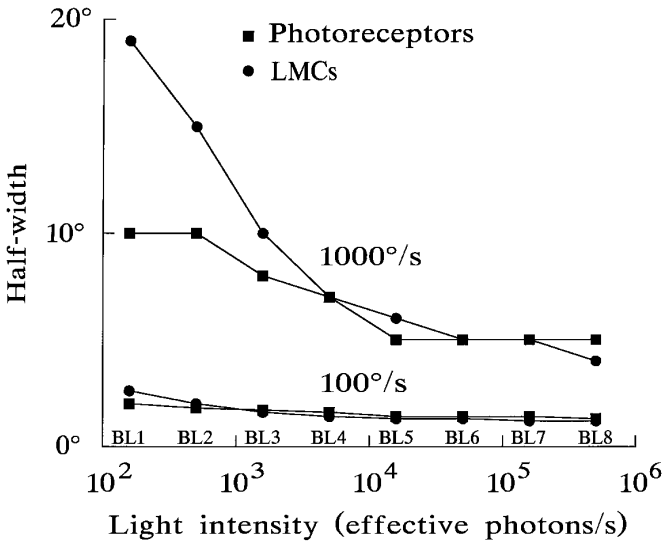

FIG. 9. Spatial half-widths of photoreceptor and LMC responses at angular velocities of 100 and 1,000°/s as a function of background light level, BL1–BL8.

mately constant spatial half-width over the entire range of facet positions.

DISCUSSION

The data presented here were made possible by our previous presentation of accurate measurements of impulse responses in photoreceptors and LMCs at a range of light intensities, as well as our demonstration that low-order Volterra series can predict the responses in these cells with fidelity (Juusola et al. 1995b). The availability of angular sensitivity data as a function of light intensity and facet location (Hardie 1979) was also crucial. Our results give the first available description of the effects of moving objects on the sensitivity and spatial resolution of photoreceptors and LMCs in the fly, taking into account the significant nonlinearity of LMC responses under light-adapted conditions. Our simulations also predict the responses of photoreceptors and LMCs under relatively natural conditions, because they use measurements made with constant contrast at varying mean light intensities, which would be close to the conditions occurring in nature.

The amplitudes of the responses to moving objects (Fig. 4) show that LMCs improve the overall ability of the eye to detect moving objects by compressing the wide range of photoreceptor responses at different light levels to a narrower range. The band-pass frequency response of LMCs (French and Järvilehto 1978b) causes a corresponding peak in sensitivity to the velocity of moving objects that is maximal in the range of 100–200°/s. This may be compared with the optimum matched-filter model of LMCs proposed by Srinivasan et al. (1990), in which response increased linearly with velocity up to ~1,000°/s. However, it should be emphasized that the present calculations do not include the effects of surround inhibition, which narrows the effective angular acceptance function and is thought to contribute to motion detection in flies (Reichardt and Poggio 1976; Srinivasan et al. 1990). It must also be emphasized that, although the peripheral visual system places limits on motion detection, the dynamics of higher motion detection systems must also be considered in predicting behavioral responses to moving stimuli.

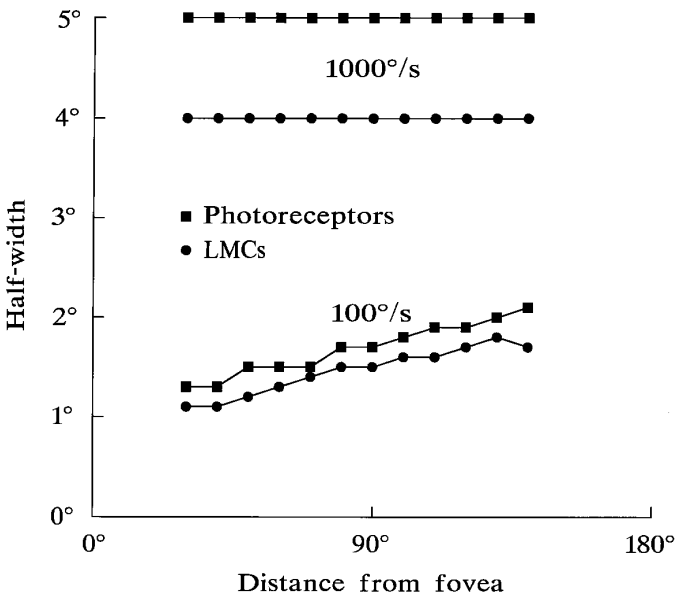

FIG. 10. Spatial half-widths of photoreceptor and LMC responses at angular velocities of 100 and 1,000°/s at background light level BL8 as a function of distance of the receiving facet from the front (fovea) of the eye.

Our results for the resolution of moving point objects by fly photoreceptors are qualitatively similar to those found for the locust eye. The two types of behavior, at low and high angular velocities, have been called the quasistatic and hyperdynamic regions, respectively (Srinivasan and Bernard 1975). A major difference between the findings in the two animals is that the transition between the low- and high-velocity regions occurred at ~20°/s in the locust, compared with ~200°/s in the fly. This reflects the much faster responses in fly photoreceptors and LMCs.

Srinivasan and Bernard (1975) also obtained an analytical expression for photoreceptor motion resolution by approximating the photoreceptor impulse response with a stretched Gaussian function, and convolving this with a Gaussian representation of the angular acceptance function. Unfortunately, the stretched Gaussian function did not give a very good fit to the actual impulse response. These impulse responses can usually be well fitted by log-normal functions (Payne and Howard 1984) or by functions based on the Gamma distribution (Wong et al. 1980), but neither of these functions can easily be convolved with the Gaussian function. For LMCs, no simple models are yet available to fit the impulse response, and even if a good analytical model were available, LMCs are distinctly nonlinear, so at least second-order convolution would be required. The digital simulations used here gave reasonably efficient estimates of the sensitivities and resolutions of the cells to moving objects, and did not require the impulse responses to be fitted by any analytical functions.

The separation of the responses into two angular velocity regions reflects the two major processes involved, light acceptance by the lens-rhabdome combination, and temporal spreading by the voltage responses of the photoreceptors and LMCs. Below ~200°/s the spatial half-width depends mainly on the Gaussian angular acceptance of light. Above this velocity, the voltage responses can no longer follow the rapid changes in intensity caused by the moving object, and the spatial response is more and more spread across the eye. Thus the temporal response of these cells not only limits the ability of the animal to follow a change in light intensity, but (probably more importantly) also limits its ability to follow a moving object or to see while moving relative to its background.

A question that immediately arises is: what angular velocities does the fly visual system experience normally? Angular velocity depends on the distance of an object from the animal, as well as the linear velocity of the object. It is easy to see that movements of a physical object, such as a human hand, very close to a fly's head could produce angular velocities exceeding 1,000°/s. Figures 6 and 8 suggest that although the movement of such an object would be detected, its form would be poorly resolved.

Another approach is to observe flies in flight, particularly when performing a difficult spatial maneuver, such as chasing other flies. This kind of observation was made by high-speed cinematography (Wagner 1986a,b; Wehrhahn 1985) and showed that both male and female flies can turn at angular velocities approaching 3,000°/s. Flies have also been made to track moving stimuli while held in a stationary position, with the tracking measured by torque production. Under these conditions, flies tracked objects moving relative to themselves at >200°/s (Reichardt and Poggio 1976; Virsik and Reichardt 1976). The size and shape of the visual stimulus was also a significant factor in both tethered flight (Virsik and Reichardt 1976) and free flight (Wagner 1986b), although widefield stimuli were relatively more effective in tethered flight and relatively less effective in free flight. The present results can only be considered in the context of small-field stimuli and are consistent with the maximum values of ~200°/s seen in tethered tracking. Male flies have specialized parts of their visual systems for tracking other flies (Wehrhahn 1985), and the present results can probably not be extended to this system. However, motion at an angular velocity of >1,000°/s must significantly compromise the resolving ability of the normal part of the fly visual system, with the spatial response being more than twice as large as when stationary.

Another question is the relationship between the present results and limitations imposed by receptor spacing. We did not assume any value for the angular spacing of photoreceptors, although some of the simulations used an unrealistically fine resolution of 0.2°. Because the spatial half-width increases with angular velocity above ~200°/s, the spatial response becomes spread across the eye and the photoreceptor spacing becomes less important. Thus spacing does not limit the resolution of objects moving above this velocity. These arguments assume that photoreceptors and facets are regularly spaced across the eye. Irregularities of receptor location can degrade the resolution of an eye significantly (French et al. 1977) and this would also apply to the detection of moving objects.

For most of the result obtained here, the ability of LMCs to resolve moving objects followed that of photoreceptors quite closely, or was better. However, this broke down at low light background levels and high angular velocities, when the slower responses of LMCs caused substantially worse resolution of moving objects. The resolution of rapidly moving objects by both types of cells was impaired at lower light levels, but for movements below ~200°/s background light level was not a major factor.

In contrast to the effects of light background, the change in angular acceptance seen in different regions of the fly eye affects the detection of slowly moving rather than rapidly moving objects. This would be understandable if the lateral regions of the eye were used more for movement detection than for the analysis of stationary objects. A similar principle can be seen in comparative visual ecology, where slowly moving insects have relatively slow photoreceptors and large facets, whereas rapidly flying insects have faster receptors and facets with smaller angular acceptance (Weckström and Laughlin 1995).

We thank I. Meinertzhagen, S. Shaw, M. Weckström, and R. Uusitalo for valuable discussion in the preparation of the manuscript.

Support for this work was provided by the Medical Research Council of Canada.

Address for reprint requests: A. S. French, Dept. of Physiology and Biophysics, Dalhousie University, Halifax, NS B3H 4H7, Canada.

Received 8 August 1996; accepted in final form 2 December 1996.

REFERENCES

EGELHAAF, M., HAUSEN, K., REICHARDT, W., AND WEHRHAHN, C. Visual course control in flies relies on neuronal computation of object and background motion. *Trends Neurosci.* 11: 351–358, 1988.

FRENCH, A. S. Phototransduction in the fly compound eye exhibits temporal resonances and a pure time delay. *Nature Lond.* 283: 200–202, 1980a.

FRENCH, A. S. The linear dynamic properties of phototransduction in the fly compound eye. *J. Physiol. Lond.* 308: 385–401, 1980b.

FRENCH, A. S. AND JÄRVILEHTO, M. The dynamic behaviour of photoreceptor cells in the fly in response to random (white noise) stimulation at a range of temperatures. *J. Physiol. Lond.* 274: 311–322, 1978a.

FRENCH, A. S. AND JÄRVILEHTO, M. The transmission of information by first and second order neurons in the fly visual system. *J. Comp. Physiol. A Sens. Neural Behav. Physiol.* 126: 87–96, 1978b.

FRENCH, A. S., SNYDER, A. W., AND STAVENGA, D. G. Image degradation by an irregular retinal mosaic. *Biol. Cybern.* 27: 229–233, 1977.

GOODMAN, J. W. *Introduction to Fourier Optics.* New York: McGraw-Hill, 1968, p. 130.

GÖTZ, K. G. Optomotorische Untersuchung des visuellen Systems einiger Augenmutanten der Fruchtfliege *Drosophila. Kybernetik* 2: 77–92, 1964.

GÖTZ, K. G. Die optischen Übertragungseigenschaften der Komplexaugen von *Drosophila. Kybernetik* 2: 215–221, 1965.

HARDIE, R. C. Electrophysiological analysis of fly retina. I. Comparative properties of R1–6 and R7 and 8. *J. Comp. Physiol. A Sens. Neural Behav. Physiol.* 129: 19–33, 1979.

HARDIE, R. C. A histamine-activated chloride channel involved in neurotransmission at a photoreceptor synapse. *Nature Lond.* 339: 704–706, 1989.

JÄRVILEHTO, M. AND ZETTLER, F. Micro-localisation of lamina-located visual cell activities in the compound eye of blowfly *Calliphora. Z. Vergl. Physiol.* 69: 134–138, 1970.

JUUSOLA, M., KOUVALAINEN, E., JÄRVILEHTO, M., AND WECKSTRÖM, M. Contrast gain, Signal-to-noise ratio and linearity in light-adapted blowfly photoreceptors. *J. Gen. Physiol.* 104: 593–621, 1994.

JUUSOLA, M., UUSITALO, R. O., AND WECKSTRÖM, M. T. Transfer of graded potentials at the photoreceptor-interneuron synapse. *J. Gen. Physiol.* 105: 117–148, 1995a.

JUUSOLA, M., WECKSTRÖM, M. T., UUSITALO, R. O., KORENBERG, M. J., AND FRENCH, A. S. Nonlinear models of the first synapse in the light-adapted fly retina. *J. Neurophysiol.* 74: 2538–2547, 1995b.

KORENBERG, M. J. Statistical identification of parallel cascades of linear and nonlinear systems. *IFAC Symp. Ident. Syst. Param. Est.* 1: 580–585, 1982.

KORENBERG, M. J. Parallel cascade identification and kernel estimation for nonlinear systems. *Ann. Biomed. Eng.* 19: 429–455, 1991.

LAUGHLIN, S. B., HOWARD, J., AND BLAKESLEE, B. Synaptic limitations to contrast coding in the retina of the blowfly *Calliphora. Proc. R. Soc. Lond. B Biol. Sci.* 231: 437–467, 1987.

MARMARELIS, P. Z. AND MARMARELIS, V. Z. *Analysis of Physiological Systems. The White Noise Approach.* New York: Plenum, 1978.

PAYNE, R. AND HOWARD, J. Response of an insect photoreceptor: a simple log-normal model. *Nature Lond.* 290: 415–416, 1984.

REICHARDT, W. AND POGGIO, T. Visual control of orientation behavior in the fly. *Q. Rev. Biophys.* 9: 311–375, 1976.

SHAW, S. R. Early visual processing in insects. *J. Exp. Biol.* 112: 225–251, 1984.

SRINIVASAN, M. V. AND BERNARD, G. D. The effect of motion on visual acuity of the compound eye: a theoretical analysis. *Vision Res.* 15: 515–525, 1975.

SRINIVASAN, M. V., PINTER, R. B., AND OSORIO, D. Matched filtering in the visual system of the fly: large monopolar cells of the lamina are optimized to detect moving edges and blobs. *Proc. R. Soc. Lond. B Biol. Sci.* 240: 279–293, 1990.

VIRSIK, R. P. AND REICHARDT, W. Detection and tracking of moving objects by the fly *Musca domestica. Biol. Cybern.* 23: 83–98, 1976.

WAGNER, H. Flight performance and visual control of flight of the free-flying housefly (*Musca domestica* L.). II. Pursuit of targets. *Philos. Trans. R. Soc. Lond. B Biol. Sci.* 312: 553–579, 1986a.

WAGNER, H. Flight performance and visual control of flight of the free-flying housefly (*Musca domestica* L.). III. Interactions between angular movement induced by wide- and smallfield stimuli. *Philos. Trans. R. Soc. Lond. B Biol. Sci.* 312: 581–595, 1986b.

WARRANT, E. J. AND MCINTYRE, P. D. Arthropod eye design and the physical limits to spatial resolving power. *Prog. Neurobiol.* 40: 413–461, 1993.

WECKSTRÖM, M. T. AND LAUGHLIN, S. B. Visual ecology and voltage-gated ion channels in insect photoreceptors. *Trends Neurosci.* 18: 17–21, 1995.

WEHRHAHN, C. Visual guidance of flies during flight. In: *Comprehensive Insect Physiology, Biochemistry and Pharmacology*, edited by G. A. Kerkut and L. I. Gilbert. Oxford, UK: Pergamon, 1985, vol. 6, p. 673–684.

WONG, F., KNIGHT, B. W., AND DODGE, F. A. Dispersion of latencies in photoreceptors and the adapting bump model. *J. Gen. Physiol.* 76: 517–537, 1980.